Available online at www.sciencedirect.com

ScienceDirect

Energy Procedia 132 (2017) 273–278

Energy Procedia

www.elsevier.com/locate/procedia

11th Nordic Symposium on Building Physics, NSB2017, 11-14 June 2017, Trondheim, Norway

Hygric property estimation of porous building materials with multiscale pore structures

Muhammad Islahuddin and Hans Janssen*

KU Leuven, Department of Civil Engineering, Building Physics Section, 3001 Leuven, Belgium

Abstract

The hygric properties of porous building materials can be numerically estimated from pore structure information. These pore structures are captured by micro-CT scanning, resulting in a virtual network of pores and throats. Such pore network models of porous building materials are typically multiscale, as building materials commonly have wide pore size ranges. In these materials, the numerous fine pores play a significant role in determining the material's hygric properties. This paper hence quantitatively studies the effect of these subsidiary pores by utilizing a multiscale pore network model.

Peer-review under responsibility of the organizing committee of the 11th Nordic Symposium on Building Physics.

Keywords: hygric property; moisture flow; pore network model; porous building material; multiscale pore structures;

1. Introduction

Building materials are continuously designed to be more sustainable and durable, in order to create healthier and more comfortable living environments. Moisture-related problems do however often appear, damaging the building materials and degrading the built constructions. Mould growth, for instance, is formed due to excessive indoor relative humidities, resultantly spoiling the aesthetic of the buildings and threatening the health of the building occupants. To avoid such problems, it is essential to predict the material's hygric behaviour, for which an accurate estimate of the hygric properties is crucial.

A series of measurements commonly has to be undertaken to estimate each moisture storage and transport. For instance, the standard desiccator test and the cup test are to determine the moisture storage and transport for the

* Corresponding author. Tel.: +32 16 32 13 26.
E-mail address: hans.janssen@bwk.kuleuven.be

1876-6102
Peer-review under responsibility of the organizing committee of the 11th Nordic Symposium on Building Physics
10.1016/j.egypro.2017.09.722

hygroscopic region, respectively. Such experiments are repetitively and sequentially performed for several samples, thus requiring a significant amount of time and effort.

The resulting data from those experiments are moreover incomplete. Neither the storage nor the transport properties in the transition zone have ever been measured completely and accurately. Moreover, neither the storage nor the transport function in the near-saturated zone have previously been investigated experimentally.

Numerical models hence come into play to potentially resolve the inadequacies found in these experimental methods. Naturally, numerical simulation can be customized to produce a complete result for the whole capillary range. Applying such approaches to porous building materials is however difficult because of the numerous micropores, excessively enlarging the virtual pore network system. This results in considerable computational expense, which hinders the analysis of such large systems.

This study hence aims at investigating the resultant effects of fine pores to the hygric properties of multiscale building materials. To this end, the topological pore network model is preferred, since its lightness enables us to work with large systems. The developed pore network model is complemented by a light and fast multiscale method to upscale the effect of subsidiary pores of multiscale materials. This multiscale numerical model can then serve as a faster, cheaper and reliable alternative approach to the experimental methods, by producing complete and accurate results.

2. Pore network model

The estimation of the hygric properties is performed using the quasi-static pore network model. Such model assumes an equilibrium flow on a network of pores and throats. This model can reliably reconstruct the moisture retention curve and the moisture permeability curve for the whole capillary pressure range. The developed model has been presented in [1], where the detailed description can be found. For completeness of this paper, only the main ideas are briefly presented here.

The moisture storage can be calculated by summing all of the liquid water present in the network: the condensed pore water and the adsorbed water film. This will give the actual amount of moisture, since the pore network is accurately sized based on the sample image. Prior to calculating the moisture content, the condensed water distribution must be determined based on the Kelvin equation, and the water film thickness in the dry pores can be estimated by the Bradley equation [2].

Once the equilibrium moisture distribution has been determined, an infinitesimal pressure difference is applied globally to two opposing boundaries. The moisture then steadily flows in liquid form in the water-filled elements, and diffuses in vapour form in the air-filled elements. In each pore, the steady-state condition implies that the masses flowing in and out of the pore are identical. This mass conservation leads to a system of linear equations $Ax = b$, where the matrix entry a_{ij} is the conductances between two pore centers i and j dictated by the moisture forms and the geometries of the channels, and the unknown x_i is the capillary pressure at pore i. Having solved the pressure field, the global flow through the in/outlet plane is subsequently calculated to further determine the permeability using the Darcy equation.

3. Hygric property estimation of multiscale pore structures

3.1. Multiscale pore network model

Porous building materials commonly have wide range of pore radii. The pore network models of building materials are however commonly unavailable, due to the complex trade-off between accuracy and size in the imaging methods. Therefore, statistically generated virtual multiscale networks A and B are used in this study, to examine the possible complexities encountered in multiscale networks. The individual image-based statistical information on each pore scale is used to generate the multiscale network in the domain of the macro network [3]. Fig. 1 (left) shows the spatial pore distribution of network A in which the fine and coarse pores are homogeneously scattered. Next to it, in the center of Fig. 1, the complex pore connectivity is displayed with an enlarged zoom. The pore size distributions of network B are presented in Fig. 1 (right). Only these selected data are presented here, due to the space limitation imposed for this paper.

Other networks containing only the coarse pores and throats are derived from these two multiscale networks to investigate the role of the microporosity. The fine pores and throats are removed based on the so-called cut-off diameter which represents the minimum diameter of the coarse elements. Simulations on these full- and coarse-scale networks will quantitatively reveal the contributions of the fine elements. Their network properties are presented in Table 1.

Table 1. Properties of the full- and coarse-scale networks. The two variants of the coarse network are determined by the cut-off diameters which are either defined from the image resolution (coarse 1) or from the size distribution (coarse 2). The data contains no isolated pores.

Properties	Network A			Network B		
	Full A	Coarse A1	Coarse A2	Full B	Coarse B1	Coarse B2
Side length [mm]	0.61	0.61	0.61	0.53	0.53	0.53
Network porosity [%]	17.32	16.14	6.87	16.89	6.35	4.13
Average coordination number [-]	3.46	2.81	2.49	2.78	2.11	2.30
Cut-off diameter [µm]	-	1.00	8.77	-	1.00	3.73
Number of pores [-]	177,467	144,319	189	2,744,582	45,819	3,457
Number of throats [-]	307,128	202,509	235	3,818,440	48,276	3,972
Number of spanning pores [-]	175,801	142,330	0	2,723,788	16,807	1,462
Number of deleted fine pores [-]	0	25,596	177,139	0	1,979,220	2,737,329
Number of deleted fine throats [-]	0	102,376	306,795	0	3,308,868	3,811,697
Number of deleted isolated pores [-]	1,170	7,552	139	261,975	719,543	3,796

3.2. Upscaling technique

The existence of the fine elements, which extremely enlarge the system, results in an excessive computational cost, even unaffordable in cases. Instead of solving the full system at once, multiscale methods efficiently upscale the effect of the subscales to the macroscale. Therefore, a cost-effective multiscale method should be implemented to simulate the large multiscale networks A and B.

The existing multiscale approaches [4–6] for quantifying the moisture behavior for the cumulated scales do not work for our topological networks, as these approaches were designed for conceptual pore network models with regular and isotropic network structures. Other multiscale approaches originating from the continuum modeling are neither (easily) applicable. Sampling the fine scale with a micro-network model at each coarse throat is an HMM (heterogeneous multiscale method) alternative to this case. Nonetheless, many issues like geometrical complexity, varying fine-scale boundary conditions, and the fine-scale representativeness are obstacles to implement such method. Domain decomposition is surely an applicable method for very large networks, with a note to handle the continuity of the sub-domain boundary conditions. However, the algebraic multigrid (AMG) is a much simpler approach and is suitable for the irregular anisotropic topological networks, due to its independency of the underlying physical structure. This method is thus implemented in this simulation.

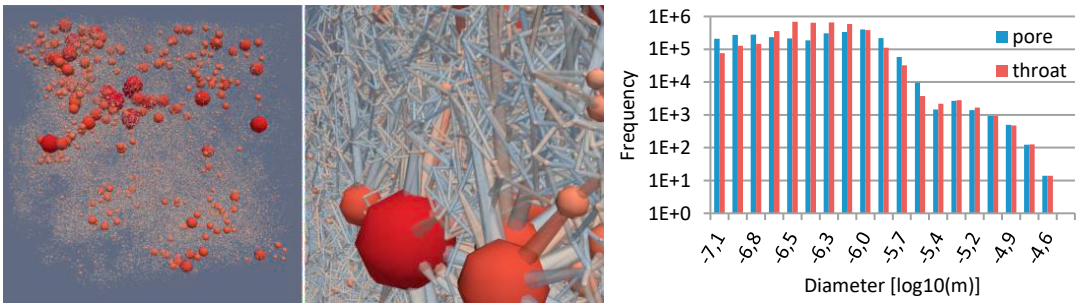

Fig. 1. (left) The spatial pore distribution and (center) the complex pore connectivity of network A; (right) the pore and throat size distributions of network B.

3.2.1. Algebraic multigrid

The algebraic multigrid (AMG) method works by generating several levels of coarse grids in which corrections to the fine level are calculated. AMG generates these coarse grids algebraically without a need of geometrical backgrounds, as it works on the matrix of a linear system $Ax = b$. The main idea of this approach is that the matrix A, due to the physical heterogeneity of the multiscale pore network, contains several levels of 'smooth error' which cannot be eliminated by single-level relaxation methods. The solution of this fine-scale relaxation process must then be corrected by the smooth error e calculated from the coarse grid $A_c e = r$, where r is the projected residual of the fine system. Note that the size of the coarse grid is smaller than that of the fine grid. Hence, the so-called restriction and prolongation operators are needed to map the fine to coarse grids and vice-versa.

The coarse grids are merely defined from the matrix entries a_{ij} which represents the conductances between two neighbouring pore centers of all throats ij in the original complete network. After deleting the insignificant entries, a subset of these matrix entries are selected as the coarse grid based on a particular coarsening method. In this coarsening process, a compromise between accuracy and memory has to be considered. A smaller coarse system is typically preferable in relation to memory requirements and calculation cost. The convergence speed is however sacrificed, since less information from the coarse level can be used to interpolate the fine-level variables. More detailed description of AMG can be found in [7,8].

3.3. Resultant effect of the fine pores

In assessing the effect of subsidiary pores to the hygric storage and transport properties, coarse networks are derived from the full-scale networks A and B. Two issues have to be addressed for such process: the cut-off diameter itself, and the removal of fine pores. First, the cut-off diameter defines the fine pores and throats as the elements having smaller diameters than this cut-off diameter. This parameter can be defined as the size that separates two different peaks in the pore size distribution. However, for porous building materials, such scale separation does not exist, because the pore size distributions are generally rather continuous. The cut-off diameter can therefore be estimated by the local minimum separating two peaks. In case of the network B, its pore size distribution (the top histogram of Fig. 2) shows that the diameter 3.7 μm (-5.43 in logarithmic scale) is the location of such local minimum. This local minimum splits the distribution into two regions: coarse (right) and fine (left), each with their own peak. The other way to define the cut-off diameter is based on the image resolution of the coarse network. This resolution determines the smallest pore size that can be captured by the image scanning, while fine pores below this size are left unidentified. This minimum diameter of the coarse network is defined as the cut-off diameter. In this simulation, the resolution-based cut-off diameter is determined from the Berea network presented in [1] as 1 μm. Second, the identified fine pores and throats should be removed in a certain way. The trivial way is to remove all of the fine pores and throats, as well as the neighbour throats of the fine pores. Removing the fine throats is obvious as throats may connect any kind of pores. However, since a pore may act as a connecting point between two neighbour throats, it may have much smaller size than that of the neighbour throats. To accommodate this issue, the fine pores connected to at least two coarse throats are preserved.

The network properties of the resulting coarse networks are listed in Table 1. The resolution-based coarse network A1 with 1 μm cut-off diameter preserves a more significant amount of porosity than retained in the coarse network A2. This preserved porosity conserves the spanning cluster that does not exist in network A2 anymore, which makes network A2 impermeable. In contrast to network A, network B1 does lose a notable amount of porosity (around 60-75% of its original porosity), which makes B1 and B2 comparable in terms of porosity. Nevertheless, both B1 and B2 preserve the spanning clusters, which make them still permeable.

The high porosity loss of B1 is confirmed by the size distribution of the full- and coarse-scale network B that is shown in Fig. 2. Around 72% and 86% of the total number of pores and throats are fine pores and throats respectively. However, it should be noted that the volumetric contribution of these numerous fine elements constitutes only 3% porosity. The biggest loss (of around 7% porosity) is attributed to a few number of isolated coarse pores, as well as their connecting throats. These isolated pore clusters are created because of the removal of the fine throats. This hypothesis is confirmed by the pore (top) and throats (bottom) size distribution of networks B and B1. Above the cut-

off diameter, the distribution of coarse pores and throats is corrected by the newly created isolated coarse clusters. While below the cut-off diameter, a few fine pores are conserved due to their connection to coarse throats.

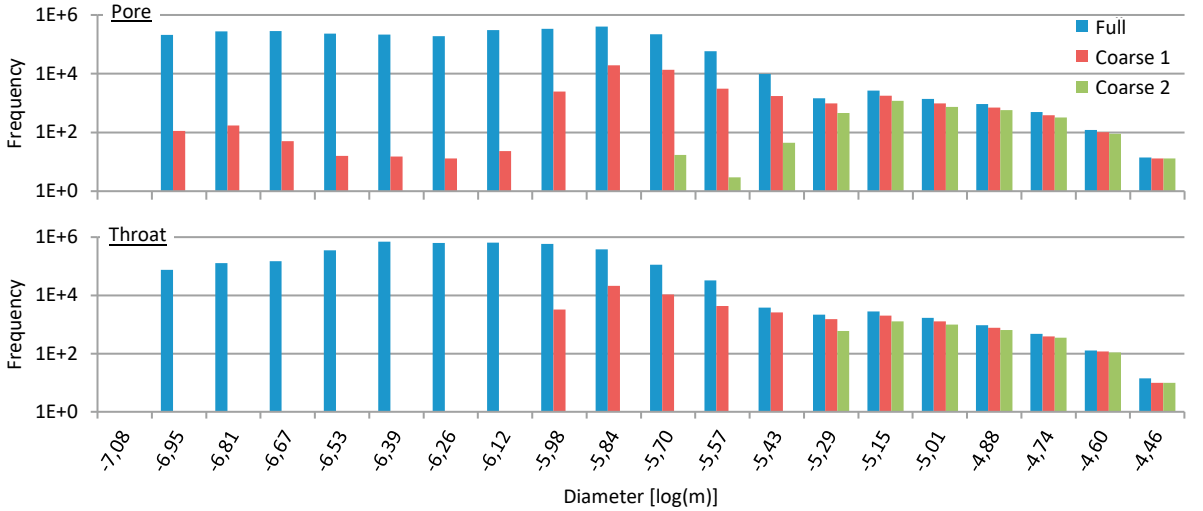

Fig. 2. The distributions of (top) pore and (bottom) throat diameters of network (blue) B and its coarse networks (red) B1 and (green) B2.

Fig. 3 shows the moisture retention and moisture permeability curves (for adsorption) on the full- and coarse-scale networks A (top) and B (bottom). The moisture retention curves (left) indicate the porosity losses of the coarse networks. The porosity preservation of A1 makes its multiscale property visible from the two slopes replicating the curve of the original multiscale network A. The slopes appearing in networks A and B occur in the capillary region, which confirms that the moisture storage is governed by the capillary condensation. Moreover, the surface adsorption does not elevate the moisture retention curves in the hygroscopic regime. Therefore, the fine pores in these multiscale networks are not significant enough to make the materials really hygroscopic.

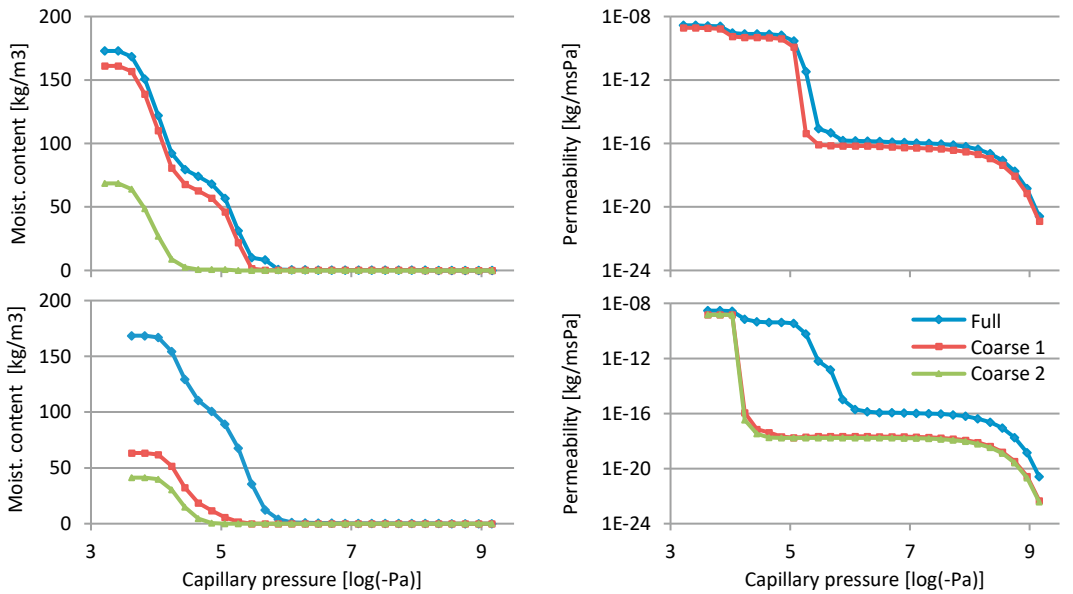

Fig. 3. (left) Moisture retention and (right) permeability curves of networks (top) A and (bottom) B, and their coarse variants.

After the rise in permeability due to the increase in vapour pressure, the permeability curve of the full-network A (Fig. 3 right) has a steep slope followed by a plateau and a small increase to the saturated condition. The moisture retention curve confirms that this steep slope is related to capillary condensation in the fine pores. Moreover, these wet fine pores form the spanning water cluster which notably increase the permeability to almost its maximum value. The following permeability is slightly rising although the moisture intake, due to condensation in the very big pores, is increased significantly. This illustrates that the remaining condensation mostly does not appear in the backbone of the spanning cluster: either in the surface clusters or the dead-end sites of the spanning cluster. The permeability of network A1 is a slightly lower than that of its full network A as a consequence of the smaller porosity. Network A2 is impermeable because of removing the fine pores that form the network's spanning cluster.

Another interesting case is found in network B in which the backbone of the spanning cluster is formed by both fine and coarse spanning clusters. Network B2, containing no fine pores, is still permeable with comparable maximum permeability as the original network B. The existence of a few fine pores in network B1 moderately increases the permeability in the transition region. However, this rise is negligible compared to the gradual but remarkable increment of the full-network permeability. The condensation appearing in the fine pores outstandingly raises the permeability, due to the formation of a spanning water cluster. This increment is achieved in two slopes, which suggests that this network can be considered as a three-scale network. The following plateau means that the invaded coarse pores belong to the surface clusters or to the dead-end sites of the spanning cluster. Finally, the last small increment is contributed by the big pores which enlarge the spanning cluster.

4. Conclusion

The effects of micropores in multiscale porous building materials have been analysed with a pore network model. Their effects depend on their spatial role as well as their porosity fraction. The fine pores may act as the main backbone of the spanning cluster, increasing the permeability several orders of magnitude once they are invaded. The removal of these fine pores leaves the network without a spanning cluster, rendering it impermeable. The fine pores may also act as a part of the spanning-cluster backbone complementary to the coarse backbone. The invasion of these subsidiary pores gradually but notably increases the permeability at smaller capillary pressures. Moreover, the inexistence of these fine pores does not result in impermeability.

Generally speaking, this quantitative study has shown that the fine pores are a central issue in both moisture storage and transport, and should thus be accounted for.

Acknowledgements

This project is supported by the FWO Odysseus grant 'Moisture transfer in building materials: analysis at the pore-scale level'. We thank Zeyun Jiang for his kind support in providing the multiscale pore network models, and Stefan Vandewalle for the fruitful discussion about the algebraic multigrid.

References

[1] M. Islahuddin, H. Janssen, Numerical estimation of isothermal moisture storage and transport properties, in: J. Grunewald (Ed.), *Proc. CESBP Cent. Eur. Symp. Build. Phys. BauSIM*, Dresden, 2016: pp. 301–308.

[2] R. Badmann, N. Stockhausen, M.J. Setzer, The statistical thickness and the chemical potential of adsorbed water films, *J. Colloid Interface Sci.* 82 (1981) 534–542. doi:10.1016/0021-9797(81)90395-7.

[3] Z. Jiang, M.I.J. Van Dijke, K.S. Sorbie, G.D. Couples, Representation of multiscale heterogeneity via multiscale pore networks, *Water Resour. Res*. 49 (2013) 5437–5449. doi:10.1002/wrcr.20304.

[4] P. King, The use of renormalization for calculating effective permeability, *Transp. Porous Media*. 4 (1989) 37–58.

[5] K. Xu, J. Daian, D. Quenard, Multiscale structures to describe porous media part I: theoretical background and invasion by fluids, *Transp. Porous Media.* 26 (1997) 51–73.

[6] A. V. Neimark, Multiscale percolation systems, *Zh. Eksp. Teor Fiz*. 96 (1989) 1386–1396.

[7] K. Stüben, An introduction to algebraic multigrid, in: U. Trottenberg, C. Oosterlee, A. Schuller (Eds.), *Multigrid*, Academic Press, London, 2001: pp. 413–532.

[8] U.M. Yang, Parallel algebraic multigrid methods - high performance preconditioners, *Numer. Solu. Partial Differ. Equ. Parallel Comput*. 51 (2006) 209–236. doi:10.1007/3-540-31619-1.